batteries

MDPI

Article

Scalable Silicone Composites for Thermal Management in Flexible Stretchable Electronics

George-Theodor Stiubianu [1], Adrian Bele [1,*], Marian Grigoras [2], Codrin Tugui [1], Bianca-Iulia Ciubotaru [1], Mirela-Fernanda Zaltariov [1], Firuța Borza [2], Leandru-Gheorghe Bujoreanu [3] and Maria Cazacu [1,*]

[1] Department of Inorganic Chemistry, "Petru Poni" Institute of Macromolecular Chemistry, Aleea Grigore Ghica Voda 41A, 700487 Iasi, Romania
[2] National Institute of Research and Development for Technical Physics, 47 Mangeron Boulevard, 700050 Iasi, Romania
[3] Faculty of Materials Science and Engineering, "Gheorghe Asachi" Technical University, 43 Mangeron Boulevard, 700050 Iasi, Romania
* Correspondence: bele.adrian@icmpp.ro (A.B.); mcazacu@icmpp.ro (M.C.)

Abstract: Hexagonal boron nitride (*h*BN) has been incorporated, as an active filler, in a customized silicone matrix to obtain high thermal conductivity composites, maintaining high flexibility and low dielectric permittivity, which are of interest for heat dissipation in energy storage systems (e.g., batteries or supercapacitors) and electronics. By the proper processing of the filler (i.e., hydrophobization with octamethylcyclotetrasiloxane and ultrasonic exfoliation) and its optimal loading (i.e., 10 wt%), composites with thermal conductivity up to 3.543 $W \cdot m^{-1} \cdot K^{-1}$ were obtained. Conductive heat flow (−280.04 W), measured in real heating–cooling conditions, proved to be superior to that of a commercial heatsink paste (−161.92 W), which has a much higher density (2.5 g/cm^3 compared to 1.05 g/cm^3 of these composites). The mechanical and electrical properties are also affected in a favorable way (increased modulus and elongation, low dielectric losses, and electrical conductivity) for applications as thermal management materials.

Keywords: silicone composites; boron nitride; batteries thermal management technology; thermal conductivity; surface hydrophobization; insulating; elastic energy; stress-strain; dielectric permittivity

check for updates

Citation: Stiubianu, G.-T.; Bele, A.; Grigoras, M.; Tugui, C.; Ciubotaru, B.-I.; Zaltariov, M.-F.; Borza, F.; Bujoreanu, L.-G.; Cazacu, M. Scalable Silicone Composites for Thermal Management in Flexible Stretchable Electronics. *Batteries* **2022**, *8*, 95. https://doi.org/10.3390/batteries8080095

Academic Editors: Pascal Venet, Karim Zaghib and Seung-Wan Song

Received: 25 July 2022
Accepted: 16 August 2022
Published: 18 August 2022

1. Introduction

Due to integration and miniaturization, modern electronics generate a high amount of heat, and its proper dissipation is essential for their protection [1]. Maintaining an optimal temperature can also improve the performance and can prevent the premature aging of supercapacitors or devices from electric and/or hybrid vehicles, based on development of a battery thermal management system. Such a system proved that it can provide a fast absorption and a best transfer of the heat generated by batteries and/or supercapacitors, maintaining an optimal operating temperature by different mechanisms of operations [2–4]. While traditional cooling with air or liquid presents some disadvantages related to space limitation or possible energy leakage, thermally conductive solid materials with or/without phase change can be an alternative [5].

Rapid heat transport is also required in the case of shape-memory alloy, SMA, consisting of SMA elements in the form of wires, strips, or particles in polymer matrices. When the built-in, pre-stressed SMA elements are heated, they undergo deformations while internal stresses are generated in the surrounding matrix, the release of which facilitates the return of the SMA to its original shape by cooling. For this, it is required for the polymer matrix to ensure rapid heat dissipation [6]. Most pure polymers used in electronics to reduce the size and weight of components while simplifying assembly, such as epoxy resins, polyimides, polystyrene, silicones, etc., have relatively low thermal conductivity (0.2–0.4 $W \cdot m^{-1} \cdot K^{-1}$) [1], which can greatly affect reliability and long-term

performance of the devices [7,8]. In general, to give polymers the ability to dissipate heat, the incorporation of thermally conductive fillers is used, such as metals or metal oxides (Al_2O_3, ZnO), aluminum or silicon nitrides, MWCNT, graphite nanoplates, carbon, ceramic materials, and so on [9,10]. An ideal filler candidate seems to be hexagonal boron nitride (*h*BN) due to, among other reasons, high thermal conductivity (185–300 $W \cdot m^{-1} \cdot K^{-1}$), superior electrical insulation properties with low dielectric constant and intrinsically low dielectric loss (0.001), low density, and oxidation stability [1,8,11]. This is a graphite-like, synthetic two-dimensional (2D) material with a high aspect ratio (ranging from 2:1 to 30:1). Unlike the latter, BN is white colored and has a wide energy band gap of up to 5.5 eV, making it an excellent insulator of high interest in nanoelectronic devices [11–14]. The geometry of *h*BN particles, such as platelets, flakes, or agglomerates, facilitates heat transfer and dissipation. The particles can be easily aligned by using appropriate formulation and processing techniques to form paths or bridges that conduct heat on their orientation directions, which are generally horizontal or vertical, thus proving to be an effective way to improve thermal conductivity [15]. By incorporating such a material as filler in polymers, composites with high thermal conductivity can be obtained. In addition to the nature of the filler, the effect obtained also depends on its quantity incorporated in the polymer, as well as on the geometry of the particles, their orientation, and compatibility with the matrix. The paraffin wax-based composite, with a loading of 20 wt% highly ordered and interconnected hexagonal boron nitride (*h*BN) networks, shows a thermal conductivity of 1.86 $W \cdot m^{-1} \cdot K^{-1}$, which is four times higher than the similar composite but with the unoriented filler and eight times higher than that of unfilled paraffin [5]. A simple modification of the surface of BN (spherical particles) with SiO_2, followed by incorporation into epoxy-silicone resin matrix, led to a material with improved thermal conductivity of 3.1 $W \cdot m^{-1} \cdot K^{-1}$, which is about 24% higher than unmodified BN particles and able to support the temperature distribution of a battery module [16]. Due to their very good insulating, mechanical and thermal properties, as well as good adhesion and ease of processing, silicone-based materials are preferred in many applications [17,18]. Silicones are a family of extremely versatile chemical compounds and are considered to be very environmentally friendly; most silicone products do not contain solvents, are non-volatile, and do not pose any danger to the ecosystem. Vulcanized silicone rubbers are not affected by weather, ozone, and UV exposure, and they are not biodegradable. They maintain their properties over a wide range of temperatures (usually from −60 °C to +250 °C) and provide protection against moisture, chemical attacks, shocks, and vibrations. Silicones are electrical insulators, usually having volume resistivity values greater than 10^{15} Ω·cm, which makes them of great interest for electronic engineering or for optimizing electric vehicle components, including battery safety. A wide range of mono or bicomponent products with different crosslinking systems and conditions that can be used, from micro-thin coatings, flexible adhesive sealants, gels, and rubbers with variable hardness, are commercially available. As with most polymers, unfilled silicones have a thermal conductivity of only about 0.2 $W \cdot m^{-1} \cdot K^{-1}$, with some special products barely reaching values exceeding up to 1.2 $W \cdot m^{-1} \cdot K^{-1}$. Recently, progress has been made on this direction, appearing on the market silicone material with thermal conductivity from 0.3 to 4.3 $W \cdot m^{-1} \cdot K^{-1}$ [19] or, more recently, 7.309 $W \cdot m^{-1} \cdot K^{-1}$ [20]. In general, those with this destination are vulcanizable by condensation or addition reactions, have brown or black colors, and most elongations are in the range of 120–250%, rarely reaching higher values [15]. Silicone, as a protective layer coupled with phase change materials (PCM), improved the performance of a thermal management system, ensuring a temperature of 48 °C on a battery and simplifying the complexity of a conventional cooling system [21].

Taking into account the above, this paper reports the results of room temperature hardening silicone formulations that incorporate different percentages of pristine BN, or which has previously been subjected to the original treatments, consisting of hydrophobization with D_4 vapors or hydrophobization with D_4, followed by exfoliation, so as to

maximize its effect of increasing thermal conductivity and optimizing the other properties of the material. The main steps and achievements are summarized in Scheme 1.

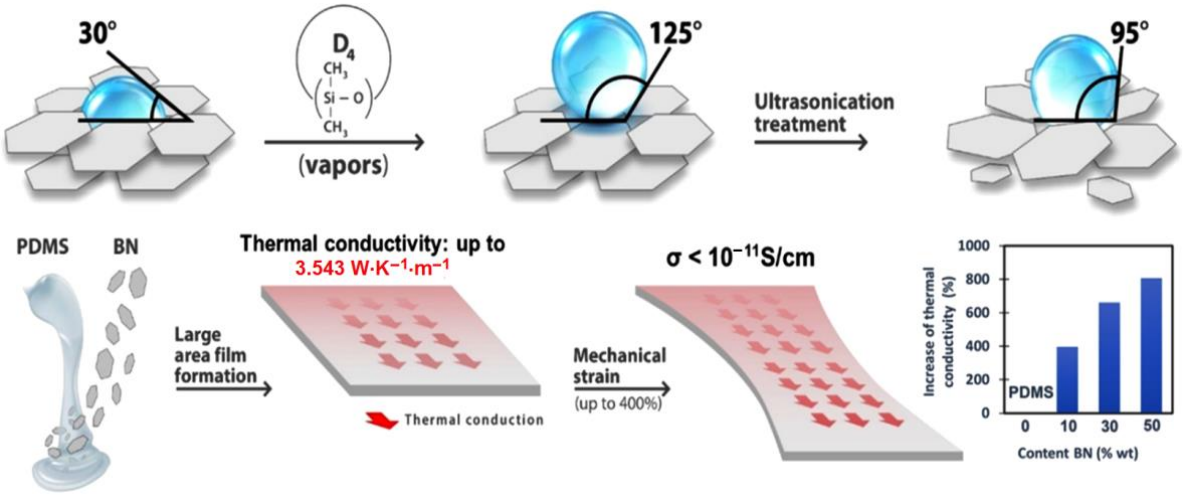

Scheme 1. Illustration of the protocol addressed in this work for obtaining composites for thermal management and their main performances obtained.

Thus, in addition to the thermal conductivity evaluation, which is the performance sought to be improved in battery thermal management systems. The materials were also assessed in terms of mechanical and electrical properties, which are of equally great interest to flexible stretchable electronics.

2. Experimental Part

2.1. Materials

The polydimethylsiloxane-α,ω-diol, PDMS, with molecular weight Mw = 63,860 g/mol and PDI = 2.2, was synthesized by ring-opening polymerization of octamethylcyclotetrasiloxane, in mass, heterogeneously catalyzed by a styrene-divinylbenzene resin functionalized with sulfonic groups (Vionit CT175), according to the procedure previously described [22]. Hexagonal Boron Nitride, *h*BN, was purchased from Sigma-Aldrich, USA, in the form of nanopowder, with the average particle size (BET) of 150 nm, Mw = 24.82 g/mol, and d = 2.29 g/mL at 25 °C (hygroscopic). Octamethylcyclotetrasiloxane (D_4), 98%, was purchased from Gelest. Tetraethylorthosilicate (TEOS), 98%, and dibutyltindilaurate (DBTDL), 95%, were purchased from Sigma-Aldrich and used as received, and isopropyl alcohol was from Chemical Company S.A. Str. Sf. Ioan 10, Iasi 700381, Romania.

2.2. Measurements

Homogenization of the mixtures to obtain composites was performed in a SpeedMixer™ DAC 150 SP, Hauschild Engineering, Waterkamp 1, 59075 Hamm, Germany, a laboratory-sized device for fast and efficient mixing materials. ATR-IR (Attenuated Total Reflectance-Infrared) spectra were registered by the Fourier Transform Infrared (FTIR) equipment (Vertex 70 Bruker, Ettlingen, Germany), which possesses a ZnSe crystal, in the 600–4000 cm^{-1} spectral region, at room temperature, with a resolution of 4 cm^{-1} and an accumulation of 32 scans. Stress–strain curves were recorded on an Instron 3365 apparatus, with an extension rate of 200 mm·min^{-1}, at room temperature, and from their linear part, the Young's modulus was determined. SEM cross-section images of the composite films fractured in liquid nitrogen were acquired on an Electron Microscope (ESEM) type Quanta 200, FEI Company, ThermoFisher Scientific Gmbh, Im Steingrund 4-6, 63303, Dreieich, Germany, operating up to 30 kV, with secondary and backscattering electrons in high vacuum mode. TEM investigation was made using a Hitachi High-Tech HT7700 Transmission Electron Microscope, Hitachi High-Technologies Corporation, 24-14 Nishi-shimbashi, 1-chome, Minato-ku Tokyo 105-8717, Japan. For the analysis, microdroplets of BN dispersions in

the solvent were deposited on the 200 mesh copper grid covered with a film of collodion and carbon, after which thesolvent was removed in vacuum. The dielectric spectra were recorded on a broadband dielectric spectrometer Novocontrol Concept 40 (Hundsangen, Germany) on a frequency range 1 Hz–10^6 Hz under normal laboratory conditions, at room temperature, on samples fixed between two plated round cooper electrodes, with a diameter of 20 mm.

A STA 449F1 Jupiter device, Netzsch, Wittelsbacherstrasse 42 Selb, 95100 Germany, was used to perform the thermogravimetric analysis (TGA). The measurements were performed in an open Al_2O_3 crucible up to 700 °C, with a heating rate of 10 °C/min, under nitrogen flow rate of 50 mL/min. The thermal conductivity was investigated using the pulse power method of the thermal transport option (TTO) of a QD PPMS-9 Physical Property Measuring System (PPMS) from Quantum Design Inc. (San Diego, CA, USA). Two-Probe Lead Configuration, using disk-shaped gold plated copper electrodes, was used for the measurements. Small cylindrical samples, with a diameter of 6 mm and a height in the range of 0.25–0.8 mm, were cut out from film samples and mounted between two gold plated copper electrodes for the measurements. Heat pulses were applied to the test samples by current passing through the gold-plated copper electrodes that adhered to the sample using an epoxy adhesive with high thermal and electrical conductivity. The thermal conductivity was measured under high vacuum (10^{-i} torr) in a steady state at room temperature. Figure 1 shows the sample assembled in the thermal conductivity measurement system holder of the TTO.

Figure 1. Sample assembled in the PPMS.

2.3. Procedure

2.3.1. Surface Treatment of the *h*BN with D_4 (BND4)

There was 5 g of BN loaded in a 100 mL two neck round-bottom flask, with mechanical stirring, after 1 mL of D_4 was added. The mixture was heated at 180 °C, for 15 h with continuous stirring, under an inert atmosphere.

2.3.2. Exfoliation of *h*BN Aggregates (BND4Ex)

The exfoliation of *h*BN was performed in liquid phase as follows: 1 g of *h*BN powder was dispersed into isopropanol (100 mL). The resulting dispersion was sonicated in Elmasonic P120 H (Elma—Hans Schmidbauer GmbH and Co. KG Gottlieb-Daimler-Str. 17 D-78224 Singen, Germany) for 1 h, at a frequency of 80 kHz, at 40 °C and, then, was left standing still to cool to room temperature for 1 h. The dispersion was transferred in another Berzelius flask, removing the decanted non-exfoliated *h*BN.

2.3.3. Preparation of PDMS-BN Composites

The 5 g of PDMS, dissolved in 10 mL of toluene, was added to pristine or differently treated BN in various percentages (0–50 wt%), 0.25 mL of TEOS, and 0.04 mL of DBTDL.

Both the polymer solution and the composite mixture were homogenized, one at a time, in a SpeedMixer^{TM} DAC 150 SP, for 1 min at 3500 rpm, after which it was poured onto the film on a Teflon substrate and allowed to vulcanize under normal laboratory conditions.

3. Result and Discussion

An in-lab prepared polydimethylsiloxane-α,ω-diol (PDMS) with Mw = 63,860 g/mol was used as a flexible matrix, for the incorporation of *h*BN, in order to obtain a composite material that mainly combines the high elasticity, mechanical flexibility, electrical insulating capacity, and weathering resistance of silicones with high thermal conductivity of BN, as well as performances of interest for electronics applications [23]. The high thermal conductivity is useful for the rapid transfer of excess heat from electronic devices to the environment. The elastic energy stored in the elastomer, in case of deformation of the assembly, due to the passage of electrical current through it for heating, would help it return after cooling to its original shape without the input of external energy [24]. In a first approach, BN was used as such. However, as would be expected and as shown in the literature [25], one of the main factors limiting heat transfer in composites with such filler is the low compatibility between BN and the matrix. To minimize this disadvantage, various filler treatments are reported in the literature, such as exfoliation, ball milling, oxidation, or treatment with organic compounds (e.g., poly(dopamine) [8] or polyrhodanine [25]) and/or silane coupling agents (e.g., γ-methacryloxypropyltrimethoxysilane, KH570 [8]), each with their own advantages and disadvantages [7,8]. Thermally conductive silicone materials on the market are of undisclosed composition, so one of the main ideas of this study was to obtain such materials with customized silicone formulation, based on own component and protocols developed in the laboratory.

3.1. Filler Processing and Characterization

Given the fact that BN is hydrophilic, due to some OH group content on the surface of the nanosheets, as shown by the IR spectrum (Figure 2), and since the matrix in which it is incorporated is a hydrophobic one, the premises for an incompatibility are created that would limit the effect of increasing the thermal conductivity induced by the filler.

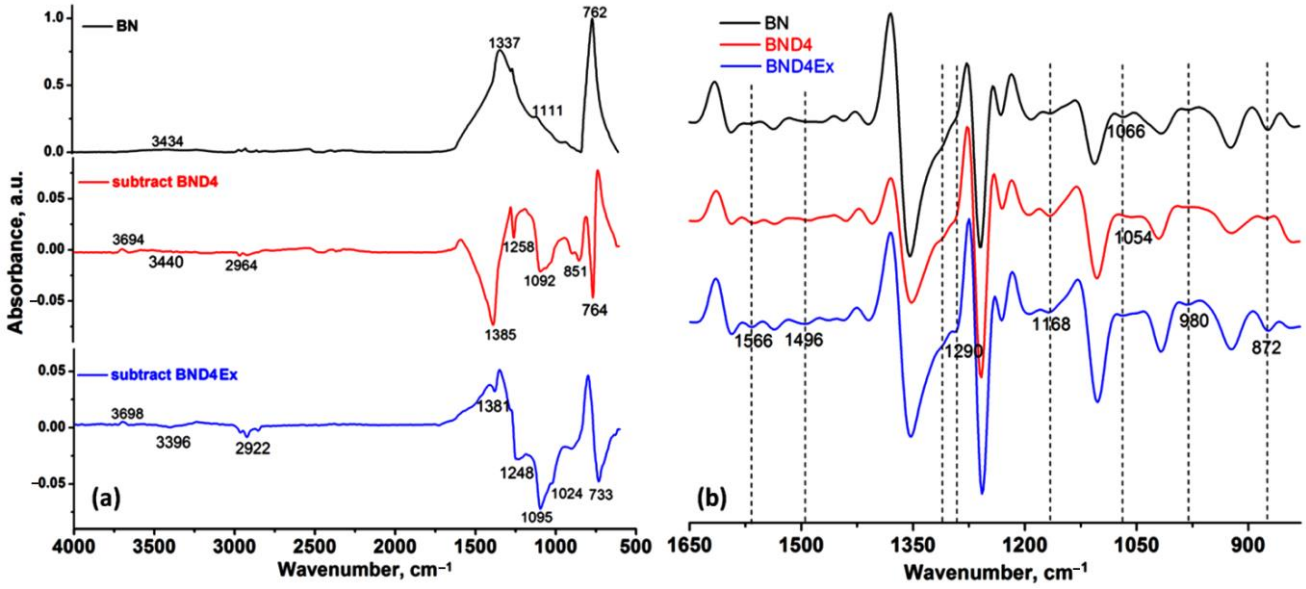

Figure 2. ATR-IR spectrum of BN, subtracted spectra of BND4 and BND4 Ex, (**a**) and the 2nd derivative of the spectra of the sample in the 1650–830 cm^{-1} (**b**).

Therefore, in the second approach to prepare composites, BN was subjected to a surface hydrophobization by treatment with octamethylcyclotetrasiloxane (D_4) in a vapor state, resulting in BND4. Hydrophobization was verified by the water drop method (placing a

water drop on a BND4 layer) (Figure 3) and by the watering test (immersion in water of a certain amount of filler powder) (Figure 4).

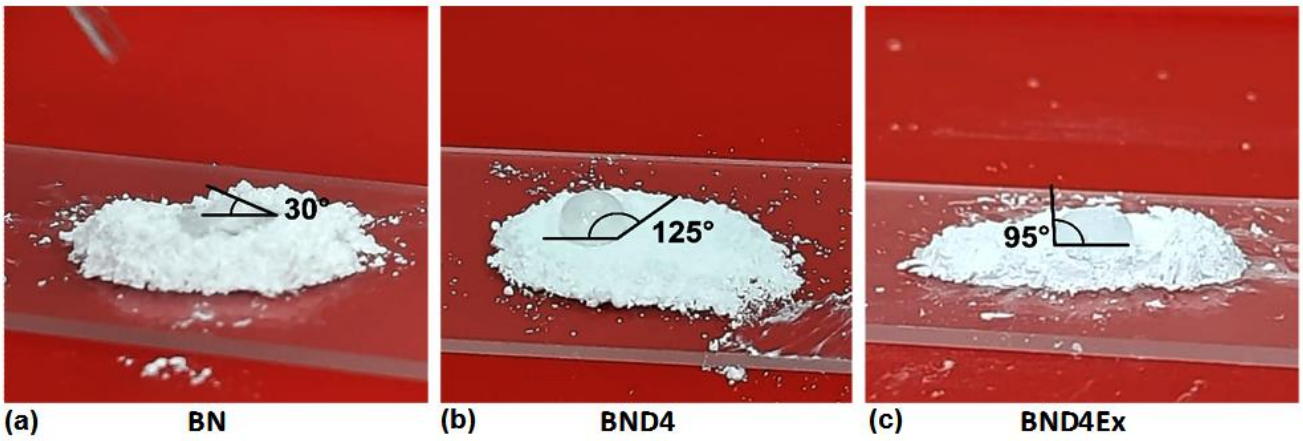

Figure 3. Photo images showing the shape of the water drop on the pristine BN powder (**a**) or treated differently: with D4 (**b**) and exfoliated after hydrophobization with D4 (**c**).

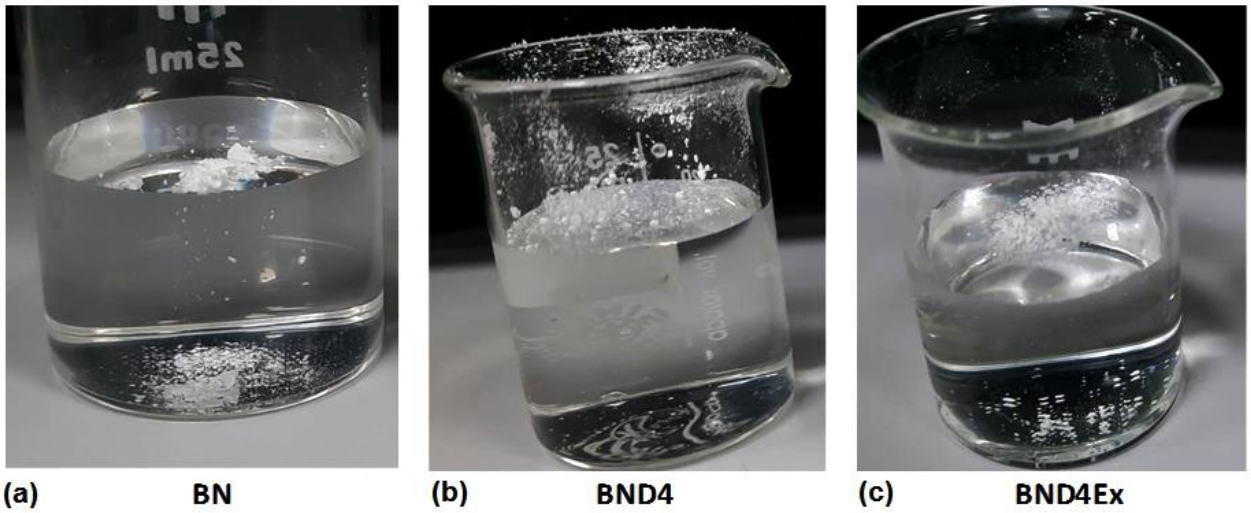

Figure 4. Images revealing the behavior, on contact, with water of the pristine BN powder (**a**) or treated differently: with D4 (**b**) and exfoliated after hydrophobization with D4 (**c**).

As can be seen, the untreated BN on which the water drop is spread immediately or the powder is deposited immediately on the bottom of the glass, BND4 remains on the surface of the water for a long time, and the water drop remains spherical on its surface. Subtracted BND4-BN spectrum (Figure 2a) confirms the presence of D_4 on the BN surface.

However, due to the polar structure of BN, nanosheets tend to stack as the TEM images (Figure 5) reveal, resulting in aggregates that could diminish the effect of incorporating them into the polymer matrix. As a result, in the third approach, BND4 was subjected to exfoliation by ultrasonication in isopropyl alcohol, resulting in BND4Ex.

The presence of D_4 after hydrophobization (BND4) and exfoliation (BND4Ex) processes was highlighted by the difference of the spectra (Figure 2a) (subtract spectra function), while the hidden and overlapped peaks of the BN, BND4, and BND4Ex in the 1650–830 cm^{-1} were found by using the second derivative of the spectra (Figure 2b). The vertical dashed lines highlight the spectral changes after the applied treatments on BN particles. Thus, the IR spectrum of BN shows two absorption bands, at 1337 cm^{-1} and 762 cm^{-1}, assigned to the B-N stretches (*h*BN). The subtracted IR spectra (subtract BND4 and subtract BND4Ex), consisting on the difference between the BN spectrum and BND4 or BND4Ex spectra, respectively, revealed the presence of the asymmetric and symmetric

stretches of C-H bonds (in Si-CH_3 groups) at 2964 and 2922 cm^{-1}, as well as 1258 and 851 cm^{-1} deformation, and the stretching vibrations of Si-CH_3 groups and Si-O-Si stretches at 1092 cm^{-1}, proving the hydrophobization of the BN particles, which stretch at 1337 cm^{-1}, is redshifted by 44–48 cm^{-1} in the treated and exfoliated samples, due to the distortion of the *h*BN lattices as a result of applied treatments [26]. After the applied treatments of the BN particles, the presence of the isolated OH groups by the band at 3694 cm^{-1} of weak intensity can be observed. The second derivative of the spectra in the 1650–830 cm^{-1} spectral region (Figure 2b) evidenced the presence of the absorption maxima characteristic for the *h*BN crystals, O-H deformation/twisting/wagging vibrations at 1290 cm^{-1}, 980, and 872 cm^{-1}, overlapped with C-H deformation vibrations from D_4. The maxima at 1168 and 1054 cm^{-1} are characteristic for Si-O stretches, being of higher intensity in BND4 and diminishing in BND4Ex [27]. Beside these, the existence of the *c*BN traces (phase mixture with *h*BN) in all samples was confirmed by the band at 1066 cm^{-1} and also proved by PXRD [28,29]. In the XRD patterns for initial, hydrophobized, and exfoliated BN particles, one can observe the presence of characteristic diffraction peaks for *h*BN at 2θ: 41.6, 43.8, 50.1, 55.1, 75.96, 76.16, and 82.15, corresponding to planes (100), (101), (102), (004), (110), and (112) (Figure 6). In addition to these majority peaks, other two lower angle peaks at 2θ: 71.35 and 87.88 are associated with the (220) and (311) planes of cubic BN (*c*BN) [27]. The same peaks are identified in all samples before and after hydrophobization and exfoliation processes, suggesting the homogeneity of the sample and the absence of the additional phase transformations during the applied treatments.

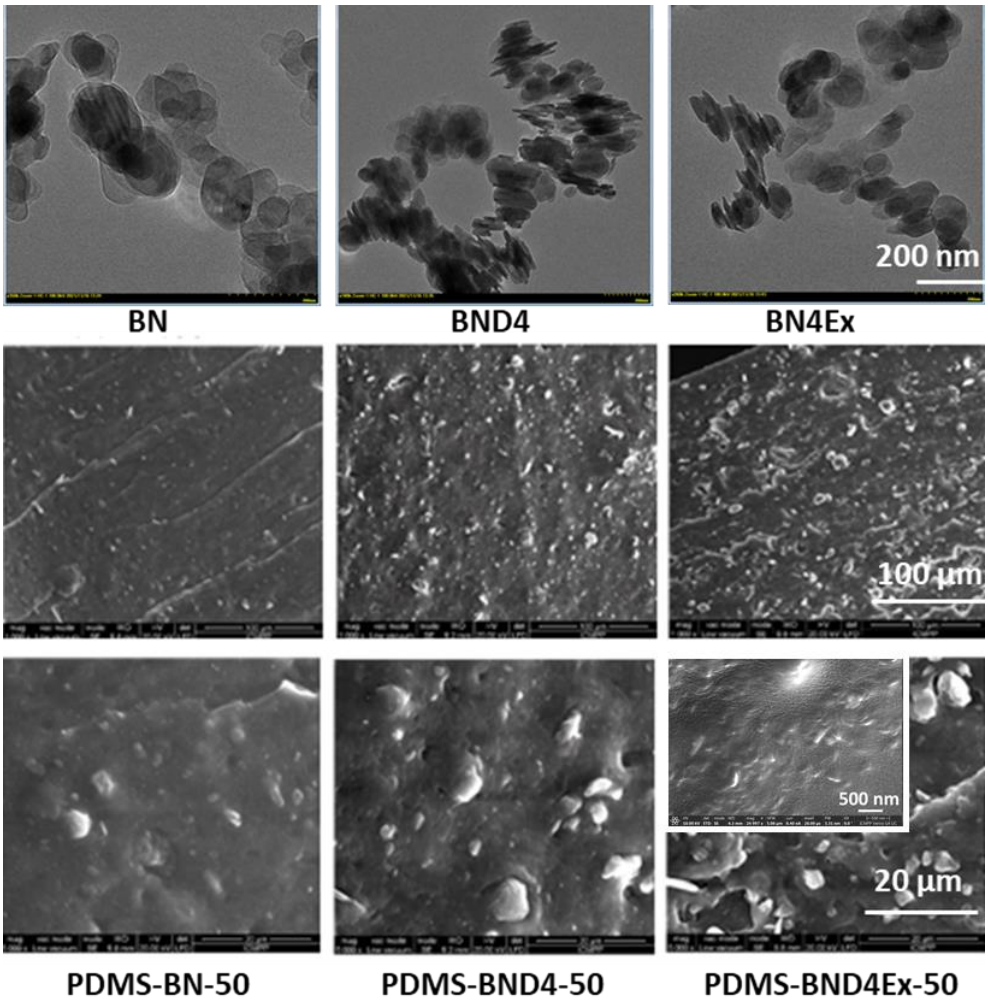

Figure 5. TEM images of the three varieties of BN (top) and SEM images of the derived PDMS-BN composites.

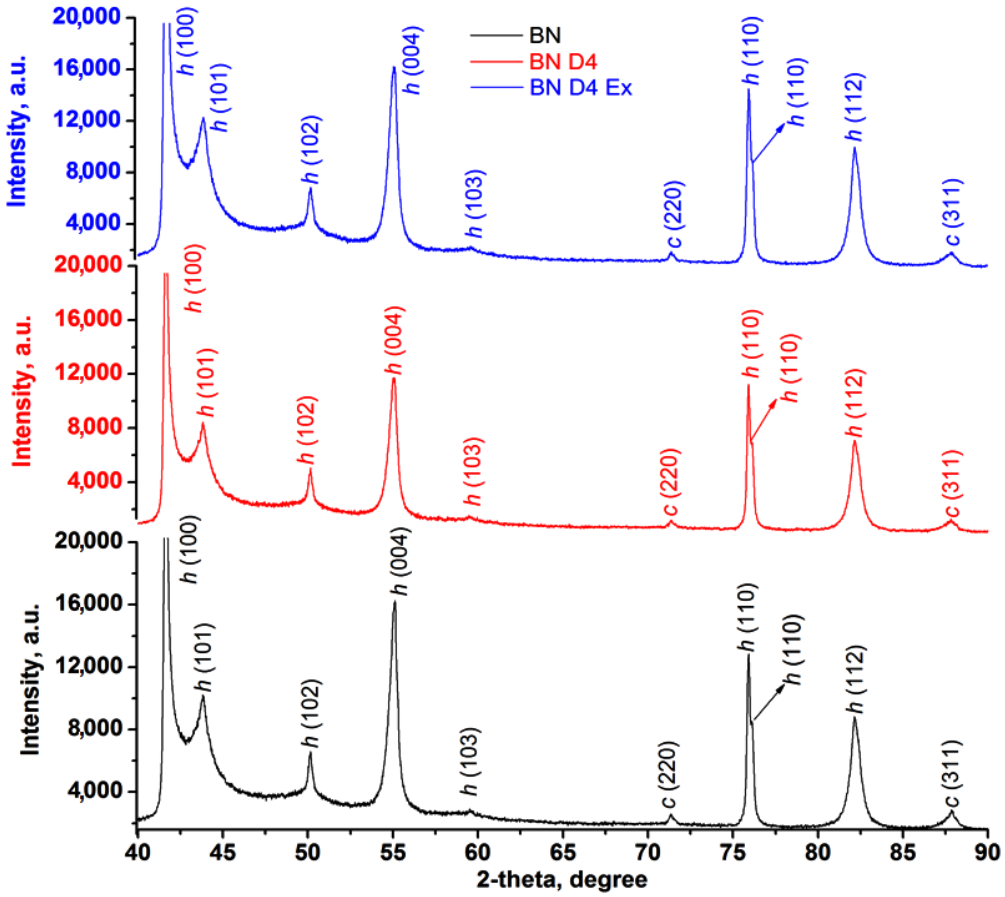

Figure 6. XRD patterns for initial, hydrophobized, and exfoliated BN particles.

Although the hydrophobicity of the powder decreased slightly (Figures 3c and 4c), TEM images indicate that exfoliation occurred (Figure 5). D_4 is still present on the BN surface, as indicated by the subtracted BND4Ex-BN IR spectrum (Figure 2).

3.2. Preparation of PDMS-BN Composites

With the three types of BN (pristine BN, BND4, and BND4ex), three corresponding series of composites were prepared, by their incorporation in PDMS matrix, in percentages of 10, 30, and 50 wt% (Table 1).

Table 1. Feed reagents amounts to obtain the series of composites.

Sample Labeling	PDMS, pph	BN, pph			DBTDL, wt%	TEOS, wt%
		BN	BND4	BND4Ex		
PDMS	100	-	-	-	0.85	5.0
PDMS-BN-10	90	10	-	-		
PDMS-BN-30	70	30		-		
PDMS-BN-50	50	50		-		
PDMS-BND4-10	90	-	10	-		
PDMS-BND4-30	70	-	30	-		
PDMS-BND4-50	50	-	50	-		
PDMS-BND4Ex-10	90	-	-	10		
PDMS-BND4Ex-30	70	-	-	30		
PDMS-BND4Ex-50	50	-	-	50		

The composite manufacturing process comprises the following steps: Step 1a—the proper amounts of boron nitride and PDMS (Table 1) were mixed using the SpeedMixer™ DAC 150 SP with toluene until a white clear solution was achieved; Step 1b—the catalyst

(DBTDL) and the cross-linker(TEOS) were added and mixed all together; Step 2a—the final mixture was drop-casted on a Teflon-coated substrate; Step 2b—after 24 h, the composite films were easily removed from the substrate and kept for 3 weeks, in laboratory conditions, before full characterization (Figure 7).

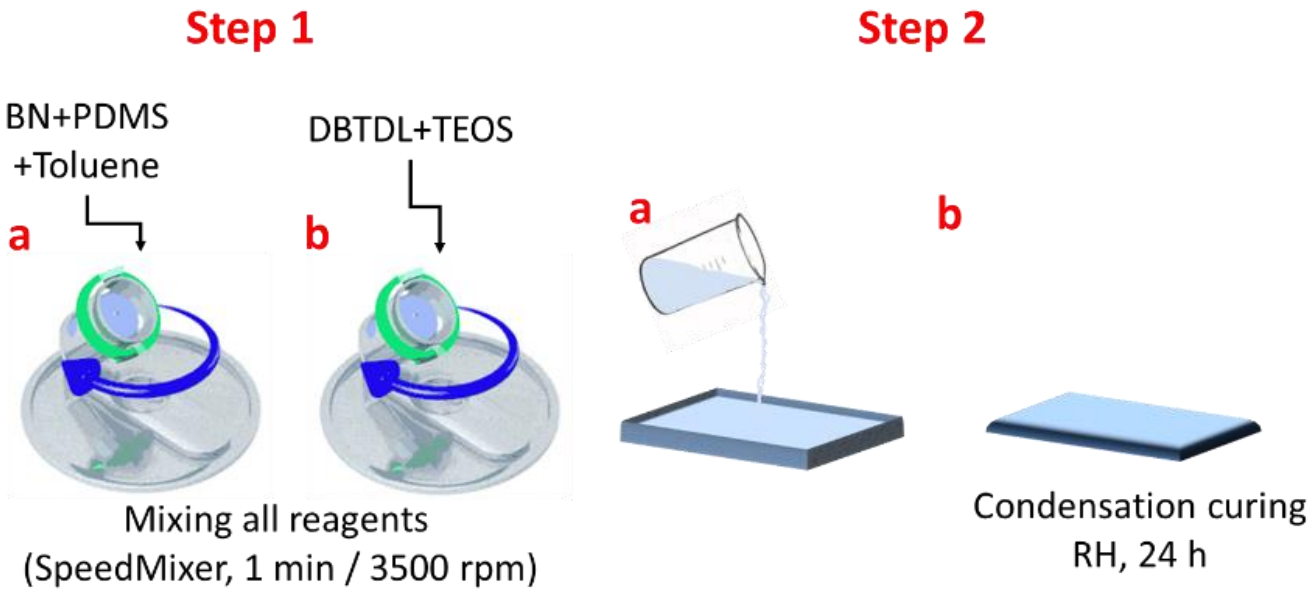

Figure 7. Manufacturing steps for obtaining silicone-based composites with BN.

3.3. Characterization of the Obtained PDMS-BN Composites

3.3.1. Analysis of the Internal Morphology of Crosslinked Composites

The SEM images in the section of crosslinked composite films and those fractured in liquid nitrogen indicate a situation somewhat announced by the TEM images of the three BN variants used as filler (Figure 5). The best dispersion of the filler seems to be in the case of composites from the PDMS-BN series. One explanation could be the involvement of OH groups on the pristine BN surface in the reaction with TEOS, in the presence of DBTDL, added to the system for condensation crosslinking of polydimethylsiloxane-α,ω-diol, which limits aggregation. In the PDMS-BND4 series, the SEM images indicate the largest and most visible filler aggregates, as indicated by the TEM image for the filler, while the PDMS-BND4Ex series is located between the two.

3.3.2. Study of Mechanical Behavior

For the use of composites in the incorporation of flexible stretchable electronics to be thermally managed, polymer composites must have adequate mechanical properties in the sense that they are flexible enough to allow deformation and sufficiently elastic so that the energy stored during deformation ensures a return to the original shape of the device. Therefore, the composite films were subjected to tensile tests by recording the stress–strain curves (Figure 8), whose main parameters are centralized in Table 2.

The analysis of the obtained data reveals that, with the increase in the filler addition, from 10 to 50%, the Young modulus increases by 3.375, 4.83, and 4.75 times in the case of the BN, BND4, and BND4Ex series, respectively, as compared to the reference sample (PDMS). Unexpectedly, the elongation at break is not negatively affected by the degree of filler loading registering even a significant increase, especially in the BND4Ex series, where it reaches 400% compared to values of maximum 250% reported in the literature for such composites [15]. Thus, BN also has a reinforcing effect, which makes the effort required for elongation to be higher. This also makes the strain energy stored during stretching high, is of greater interest in composites with SMA, and facilitates the latter's easier return to its original shape after the heat dissipation [30]. Thus, in all three series, the accumulated elastic energy increases with the filler load, but distinctly, the values are much higher in the

case of the PDMS-BND4Ex series, where it reaches the value of 33 kJ/m^3, at a 50wt% load with BN, compared to 3 kJ/m^3 in the case of pure PDMS (11 times higher).

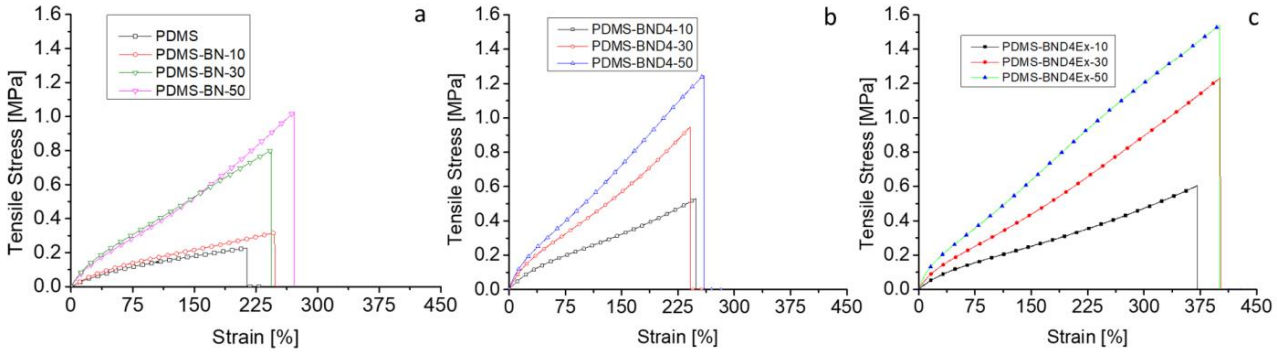

Figure 8. Stress–strain curves for the three composite series: (**a**)—with the pristine BN powder; (**b**)—with BN treated with D4; (**c**)—with BN treated with D4 and exfoliated.

Table 2. The main mechanical and dielectric parameters estimated based on stress–strain curves and dielectric spectra.

Sample	Mechanical Data (ASTM D 412-06a)			Dielectrical Data (at 1 Hz)				UTT [h]
	Sm [a], %	Y [b], MPa	Tnm [c], MPa	ε_r [d]	E″ [e]	Σ [f], S/cm	Cp [g], F	kJ/m^3
PDMS	213	0.24	0.22	3	0.25024	1.04×10^{-13}	8.15×10^{-12}	3.0
PDMS-BN-10	135	0.4	0.23	4.2	0.04638	2.63×10^{-14}	6.08×10^{-12}	1.8
PDMS-BN-30	270	0.7	1.02	4.1	0.18628	1.06×10^{-13}	6.82×10^{-12}	13.5
PDMS-BN-50	245	0.81	0.8	4.4	0.05216	2.96×10^{-14}	6.21×10^{-12}	10.7
PDMS-BND4-10	250	0.25	0.52	5.1	0.00277	1.38×10^{-11}	4.81×10^{-12}	4.5
PDMS-BND4-30	240	0.88	95	4.8	0.00123	6.18×10^{-12}	7.85×10^{-12}	11.5
PDMS-BND4-50	260	1.16	1.24	4.6	0.05072	2.88×10^{-14}	7.84×10^{-12}	16.5
PDMS-BND4Ex-10	370	0.38	0.6	3.8	6.88×10^{-4}	3.44×10^{-12}	9.47×10^{-12}	11.3
PDMS-BND4Ex-30	400	0.7	1.23	3.8	4.65×10^{-4}	2.33×10^{-12}	7.73×10^{-12}	24.3
PDMS-BND4Ex-50	400	1.14	1.53	3.6	0.00234	1.17×10^{-11}	7.51×10^{-12}	33.0

[a] Tensile strain (values given at break); [b] Young's modulus (calculated at 5 % Sm); [c] Tensile stress (values given at break); [d] Dielectric permittivity; [e] Dielectric loss; [f] Electrical conductivity; [g] Electrical capacity; [h] Ultimate tensile toughness (Elastic energy stored during elongation).

3.3.3. Study of Dielectric Behavior

For thermal management, the materials must have dielectric permittivity and dielectric losses as low as possible. The dielectric spectra, recorded at room temperature in the range 1–10^6 Hz, indicate insignificant variations, with frequency in the PDMS-BN and PDMS-BND4 series (Figure 9). In the PDMS-BND4Ex series, a low-frequency region can be distinguished (from 0.1 Hz to 10 Hz), where ε' slightly decreases (e.g., from 4.4 to 3.8 in the case of PDMS-BND4Ex-10), and after that, it remains mostly constant.

The behavior in the low-frequency region is attributed to electrical polarization phenomena, such as interfacial or electrode polarization [31,32]. The highest values of ε' (4.5–5.1) are recorded in the case of the PDMS-BND4 series, while the lowest are in the case of the PDMS-BND4Ex series. Although within the same series, the differences between the values of ε' are very small, it may be noted that, in the PDMS-BN series, the composite with 50 wt% BN has, as expected, the highest value of ε', while in the other two series, the sample with this degree of filler loading has the lowest value of ε'. However, the values of the dielectric loss remain very low, decreasing in the order of BN > BND4 > BND4Ex, with the latter series being of the order of 10^{-4}, which is a desirable property for thermally conductive materials. The electrical conductivity shows the lowest values for the PDMS-BN series (e.g., 2.63×10^{-14} for sample PDMS-BN-50), while the highest values are for the PDMS-BND4Ex series (e.g., 1.17×10^{-11} S/cm for the PDMS-BND4Ex-50 sample),

indicating that, as is logical, the delamination and better dispersion of BN leads to the increase in conductivity. However, all values remain below 10^{-11} S/cm, i.e., in the field of insulators. Electrical capacity or electrical charge storage is of the order of 10^{-12} F compared to 10^{-5}–10^{-4} F, as the ceramics have [33], which, again, corresponds to insulating materials.

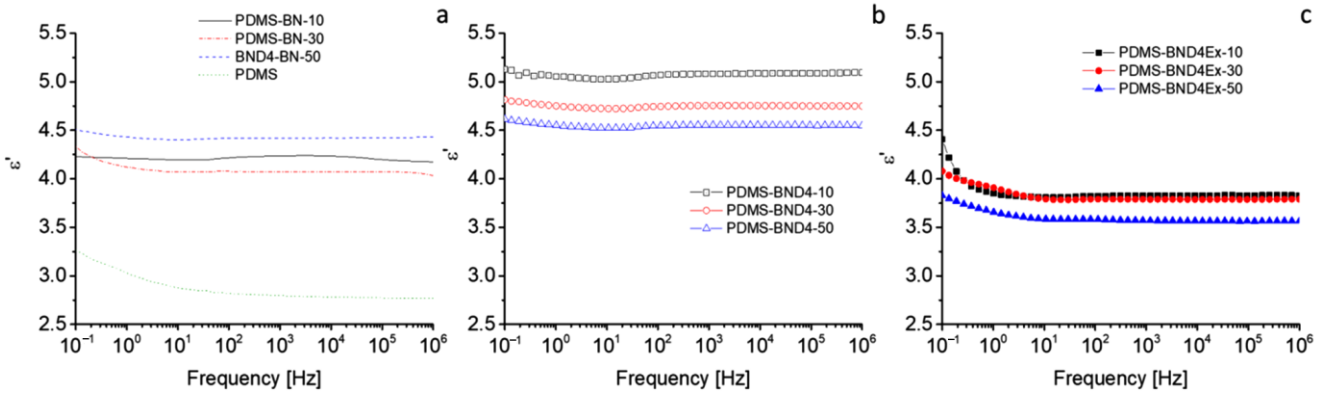

Figure 9. Dielectric spectra of the three composite series: (**a**)—with the pristine BN powder; (**b**)—with BN treated with D4; (**c**)—with BN treated with D4 and exfoliated.

3.3.4. Thermal Conductivity Assessment

The composite materials approached in this study are based on two components with increased thermal stability: silicones, known to be stable up to at least 300 °C [34], and *h*BN platelets, with reported thermal stability of up to ~1000 °C [35]. The results of the thermogravimetric analysis, performed for the PDMS-BND4ex-10 sample (Figure 10(top)), indicate a stability of the sample up to 334 °C. Thermal conductivity was measured using the pulse power method of the thermal transport option (TTO) system of the PPMS equipment (Figure 1). This system measures the ability of a material to conduct heat by monitoring the temperature drop in the sample, as a known amount of heat passes through the sample [36]. The values obtained are presented in Table 3.

Table 3. Thermal parameters of the composites.

Composite Sample	Thermal Conductivity, $W \cdot K^{-1} \cdot m^{-1}$	Conductance, $W \cdot K^{-1}$	Reference
PDMS	0.082		This study
PDMS-BN-10	1.887	0.012	This study
PDMS-BN-30	2.062	0.013	
PDMS-BN-50	2.753	0.018	
PDMS-BND4-10	1.091	0.007	This study
PDMS-BND4-30	1.675	0.011	
PDMS-BND4-50	1.994	0.013	
PDMS-BND4Ex-10	3.543	0.023	This study
PDMS-BND4Ex-30	2.259	0.014	
PDMS-BND4Ex-50	2.018	0.013	
CPCM *	1.968	-	[13]
SCPCM **	2.899	-	[13]

* composite phase change material (CPCM) based on polyethylene glycol and expanded graphite without BN. ** silicone grease/composite phase change material (SCPCM) based on polyethylene glycol, expanded graphite and BN.

As can be seen, the highest values of thermal conductivity (2.018 and 3.543 $W \cdot K^{-1} \cdot m^{-1}$) are recorded in the PDMS-BND4Ex series, values which are comparable—or higher than—those reported for composite phase change materials (CPCMs), based on polyethylene glycol and expanded graphite, with or without BN having 2.899 $W \cdot K^{-1} \cdot m^{-1}$ and 1.968 $W \cdot K^{-1} \cdot m^{-1}$, respectively [10]. This, coupled with the lowest values of dielectric loss and the highest values of elastic energy stored during elongation, indicates the BND4Ex preparation protocol, as appropriate for the purpose of this study. In the first two series, the thermal conductivity

increases with the degree of filler loading, although the values are slightly lower than in the series based on BND4Ex. This is because, in the case of the PDMS-BN series, although the dispersion of the filler is better, the incompatibility due to the surface polar groups (OH) with the hydrophobic matrix is maintained, while the even lower thermal conductivity values in the PDMS-BND4 series are attributed to filler agglomeration (Figure 5). This filler behavior could also explain the decrease in the thermal conductivity, with the increase in the loading degree in the PDMS-BND4Ex series, in which a loading degree of 10% seems to be optimal.

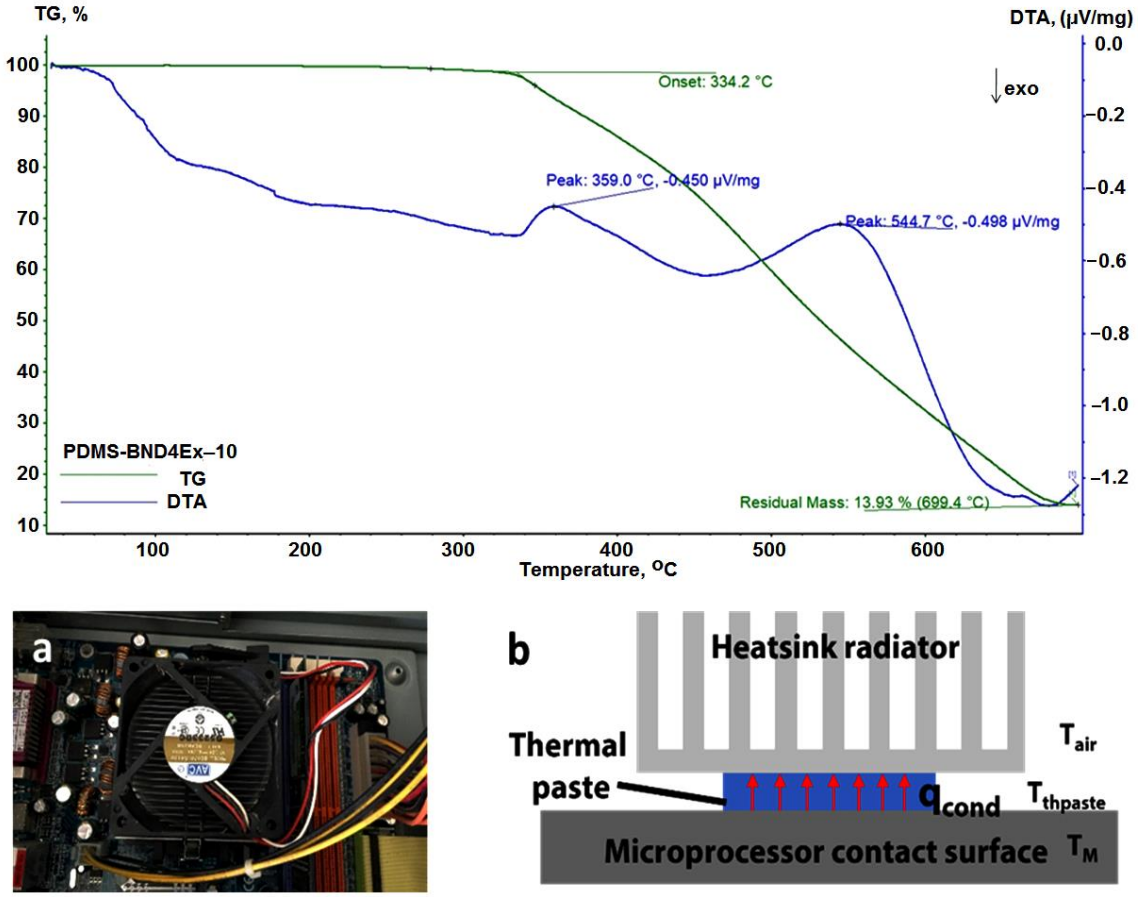

Figure 10. Thermogravimetric curve for the PDMS-BND4Ex-10 (**top**); top picture of the heatsink setup (**a**); schematics of the cooling setup with thermal paste (**b**) (**down**).

Given the relatively low degree of filler loading and the ease of preparation, the values obtained in all cases are quite high, much higher, or at the level of some reported in the literature, such as 0.58 $W \cdot K^{-1} \cdot m^{-1}$ for a commercial two-component silicone rubber (HY -9310), charged with 30 wt% *h*BN and vulcanized at 60 °C 24 h [11] or 0.515 $W \cdot K^{-1} \cdot m^{-1}$ for a silicone with unspecified characteristics incorporating 30 wt% BN exfoliated by the jet cavitation method and vulcanized at 150 °C [17] or, in case of a composite material, based on silicone grease, polyethylene glycol matrix combined with carbon, and BN fillers with a value of thermal conductivity of 2.899 $W \cdot K^{-1} \cdot m^{-1}$ [10]. For a matrix somewhat similar to the one presented in this paper, consisting of silicone, vulcanizable by condensation at room temperature but filled with a larger amount of BN (70 phr), mixed with 6 phr nanodiamond (ND) treated on the surface with 3-(trimethoxyslyl)propyl methacrylates, and values of thermal conductivity up to 0.82 $W \cdot K^{-1} \cdot m^{-1}$ are reported [37]. Higher values of thermal conductivity up to 2.632 $W \cdot K^{-1} \cdot m^{-1}$ (18 times higher than the matrix), for example, were reported in the case of a silica-reinforced silicone-based composite loaded with 60 wt% BN, as mixture of micro and nano particles, and peroxide crosslinking at 175 °C at a pressure of 10 MPa [38]. A value of 5.4 $W \cdot K^{-1} \cdot m^{-1}$ has been reported for a very high molecular weight

silicone, loaded with 150 phr BN, treated with vinyltrimethoxysilane as a compatibilizing agent, vertically aligned, and vulcanized at high temperature and pressure [39]. Very recently, a very high value of the thermal conductivity, 7.309 $W \cdot K^{-1} \cdot m^{-1}$, is reported for a boron nitride nanosheets/cellulose nanocrystals/polydimethylsiloxane (SYLGARD184) composite [20]. However, the silicone formulation addressed in our work is a simple one, which can be scaled easily without requiring material additions or high energy consumption for crosslinking.

The thermal conduction efficiency of the obtained composites was also tested for heat conduction and cooling, in real conditions, with an active radiator equipped with a 65 mm, 8.4 W fan, model DE07015B12U (Figure 10a).

The test was performed with an AMD Athlon 64 processor, 3200+, 2.01 GHz, 512 MB RAM. The composites tested were PDMS-BND4Ex-10 (Figure 11) and PDMS-BND4Ex-50, comparing the results with those of the commercial heatsink paste (Figure 11) in the cooling setup of the microprocessor. All thermal pastes were placed between the microprocessor contact surface and the heatsink radiator (Figure 10b).

The atmospheric conditions in the test laboratory were 24.8 ± 0.2 °C and 29–30% RH. The temperature measurements of the cooling surfaces were performed with an infrared camera (FLIR C2). The temperature of the heatsink contact surface with the thermal paste was measured, as well as that of the microprocessor contact surface with the thermal paste and that of the heatsink radiator, before the test and after the microprocessor run, for one hour (Figure 11).

The values of conduction heat flux, through the materials tested as thermal conductors, were also estimated by using the following equations:

- ***Commercial thermal paste:***

$$q_{cond} = -k_{thpaste} \times A \frac{T_M - T_{thpaste}}{\Delta x} = -4 \times 0.0016 \times \frac{323.1 - 297.8}{0.001} = -161.92 \text{ W}$$

where: q_{cond} = heat transferred from the microprocessor via conduction (calculated using Fourier's Law [34]); $k_{thpaste}$ = the thermal conductivity of the thermal paste [W/m·K]; Δx = the thickness of the layer of thermal paste (0.001 m = 1 mm); T_M = temperature of the microprocessor side (K); $T_{thpaste}$ = temperature of the thermal paste (K); A = area of contact with thermal paste, in m^2 (4 × 4 cm). The temperature of the microprocessor was estimated from the temperature of the hot layer of thermal paste at the end of the test.

- ***PDMS-BND4Ex-10 as thermal paste:***

$$q_{cond} = -k_{PDMS-BND4Ex-10} \times A \frac{T_M - T_{thpaste}}{\Delta x} = -3.543 \times 0.0016 \times \frac{323.1 - 297.8}{0.0005} = -280.04 \text{ W}$$

where: q_{cond} = heat transferred from the microprocessor via conduction (calculated using Fourier's Law [40]); $k_{PDMS\text{-}BND4Ex\text{-}10}$ = the thermal conductivity of the thermal paste [W/m·K]; Δx = the thickness of the layer of PDMS-BND4Ex-10 as thermal paste (0.0005 m = 0.5 mm); T_M = temperature of the microprocessor side (K); $T_{thpaste}$ = temperature of the layer of PDMS-BND4Ex-10 (K); A = area of contact with thermal paste, in m^2 (4 × 4 cm). The temperature of the microprocessor was estimated from the temperature of the hot layer of PDMS-BND4Ex-10 at the end of the test.

- ***PDMS-BND4Ex-50 as thermal paste:***

$$q_{cond} = -k_{PDMS-BND4Ex-50} \times A \frac{T_M - T_{thpaste}}{\Delta x} = -2.018 \times 0.0016 \times \frac{314.8 - 303}{0.0005} = -76.2 \text{ W}$$

where: q_{cond} = heat transferred from the microprocessor via conduction (calculated using Fourier's Law [40]); $k_{PDMS\text{-}BND4Ex\text{-}50}$ = the thermal conductivity of the thermal paste [W/m·K]; Δx = the thickness of the layer of PDMS-BND4Ex-50 as thermal paste

(0.0005 m = 0.5 mm); T_M = temperature of the microprocessor side (K); $T_{thpaste}$ = temperature of the layer of PDMS-BND4Ex-50 (K); A = area of contact with thermal paste (4 × 4 cm). The temperature of the microprocessor was estimated from the temperature of the hot layer of PDMS-BND4Ex-50 at the end of the test.

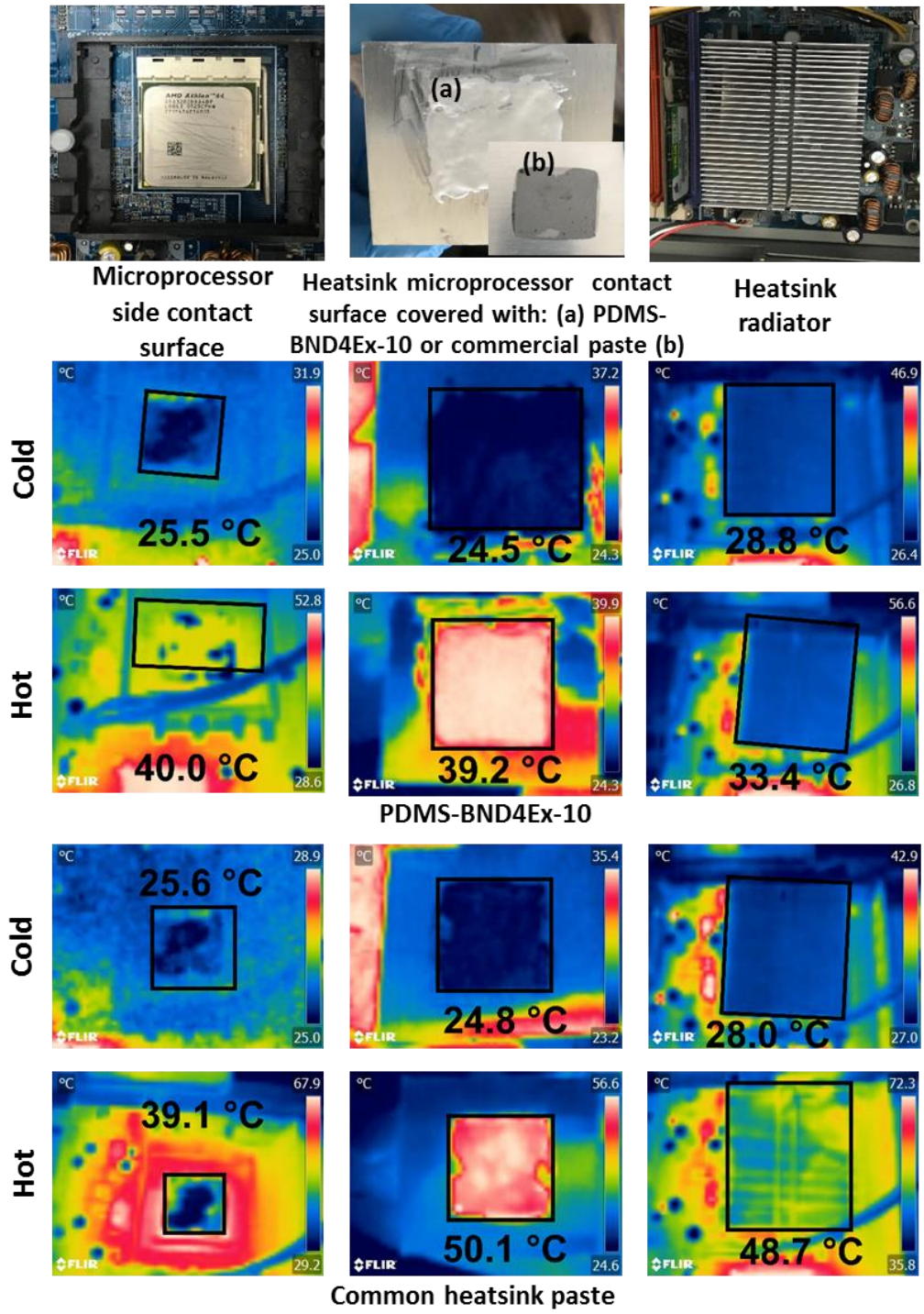

Figure 11. IR camera images and temperatures of the cooling surfaces tested for heat conduction of PDMS-BND4Ex-10 composite, as compared with commercial heatsink paste.

The conduction heat flux results show the best value for the case when PDMS-BND4Ex-10 was used as thermal paste, with a heat flux of −280.04 W, improved compared to the heat flux of the commercial thermal paste of −161.92 W. Additionally, the composite based on silicone with boron nitride has a significant advantage in terms of weight of material, with

a density of 1.05 g/cm^3, relative to the density of the commercial thermal paste with metal particles, with a density of 2.5 g/cm^3.

4. Conclusions

A relatively low molecular weight, PDMS was used as a matrix for the incorporation of *h*BN, in order to obtain composite materials useful for the thermal management of flexible electronics, but also for energy storage systems (batteries and supercapacitors). *h*BN was incorporated in three variants: as such (pristine), hydrophobized by treatment with D_4 in vapor state, and hydrophobized and exfoliated by ultrasonication in isopropyl alcohol. These three varieties of *h*BN were incorporated in percentages of 10, 30, and 50 wt% in the silicone matrix by homogenization in a SpeedMixer, with the mixtures, then, being processed in the form of films and crosslinked at room temperature. The filler was found to significantly influence the material properties under investigation, acting as a mechanical strengthening material, as well as a dielectric permittivity and thermal conductivity enhancer. Although the increased dielectric permittivity is not of interest for the studied intended application, its values proved to be very good as material with very low dielectric losses. The way the filler is conditioned plays an important role in directing these properties. The critical aspects are the compatibility with the matrix and the prevention of the agglomeration of the filler. The optimal solution found seems to be the use of hydrophobized and, subsequently, exfoliated BN (BND4Ex) as a filler in a low degree of loading in the polymer matrix, at 10 wt% obtaining a value of thermal conductivity of 3.543 $W \cdot K^{-1} \cdot m^{-1}$, and at the level of the highest reported values in the literature for such systems.

This composite also showed a higher capability for heat conduction and cooling in real conditions, as compared with commercial heatsink paste.

Author Contributions: Conceptualization, data curation, methodology G.-T.S.; data curation, investigation; writing-original draft, A.B.; investigation, M.G.; investigation, data curation, C.T.; investigation, data curation, B.-I.C. and M.-F.Z.; validation, funding acquisition, F.B.; validation, L.-G.B.; conceptualization, writing-original draft, writing-review & editing, project administration, funding acquisition, M.C. All authors have read and agreed to the published version of the manuscript.

Funding: This work was supported by a grant of the Romanian Ministry of Research, Innovation and Digitization, CNCS/CCCDI–UEFISCDI, project number PN-III-P2-2.1-PED-2019-4138, within PNCDI III (Contract 321PED/2020, SMAMEM).

Institutional Review Board Statement: Not applicable.

Informed Consent Statement: Not applicable.

Data Availability Statement: Not applicable.

Acknowledgments: Thanks to Andrei Dascalu for recording the XRD diffractograms.

Conflicts of Interest: The authors declare no conflict of interest.

References

1. Zhao, L.; Shi, X.; Yin, Y.; Jiang, B.; Huang, Y. A self-healing silicone/BN composite with efficient healing property and improved thermal conductivities. *Compos. Sci. Technol.* **2020**, *186*, 107919. [CrossRef]
2. Li, X.; Huang, Q.; Deng, J.; Zhang, G.; Zhong, Z.; He, F. Evaluation of lithium battery thermal management using sealant made of boron nitride and silicone. *J. Power Sources* **2020**, *451*, 227820. [CrossRef]
3. Raghavendra, K.V.G.; Vinoth, R.; Zeb, K.; Muralee Gopi, C.V.V.; Sambasivam, S.; Kummara, M.R.; Obaidat, I.M.; Kim, H.J. An intuitive review of supercapacitors with recent progress and novel device applications. *J. Energy Storage* **2020**, *31*, 101652. [CrossRef]
4. Al Sakka, M.; Gualous, H.; Van Mierlo, J.; Culcu, H. Thermal modeling and heat management of supercapacitor modules for vehicle applications. *J. Power Sources* **2009**, *194*, 581–587. [CrossRef]
5. Wang, Z.; Zhang, K.; Zhang, B.; Tong, Z.; Mao, S.; Bai, H.; Lu, Y. Ultrafast battery heat dissipation enabled by highly ordered and interconnected hexagonal boron nitride thermal conductive composites. *Green Energy Environ.* 2022; *in press*. [CrossRef]

6. Gururaja, M.N.; Hari Rao, A.N. A Review on Recent Applications and Future, Prospectus of Hybrid Composites. *Int. J. Soft Comput. Eng.* **2012**, *1*, 352–355.
7. Han, W.; Chen, M.; Li, W.; Li, Y.; Ge, C.; Zhang, X. Solvent-assisted encapsulation of boron nitride in polystyrene for high-efficient heat dissipation. *Polym. Test.* **2021**, *102*, 107325. [CrossRef]
8. Yang, D.; Ni, Y.; Kong, X.; Gao, D.; Wang, Y.; Hu, T.; Zhang, L. Mussel-inspired modification of boron nitride for natural rubber composites with high thermal conductivity and low dielectric constant. *Compos. Sci. Technol.* **2019**, *177*, 18–25. [CrossRef]
9. Liu, Z.; Huang, J.; Cao, M.; Jiang, G.; Hu, J.; Chen, Q. Preparation of Binary Thermal Silicone Grease and Its Application in Battery Thermal Management. *Materials* **2020**, *13*, 4763. [CrossRef]
10. Wu, T.; Hu, Y.; Liu, X.; Wang, C. Effect Analysis on Thermal Management of Power Batteries Utilizinga Form-Stable Silicone Grease/Composite Phase Change Material. *ACS Appl. Energy Mater.* **2021**, *4*, 6233–6244. [CrossRef]
11. Zhang, Y.; Huang, J.; Cao, M.; Du, G.; Liu, Z.; Li, W. Preparation of Boron Nitride and Silicone Rubber Composite Material for Application in Lithium Batteries. *Energies* **2021**, *14*, 999. [CrossRef]
12. Lee, W.; Kim, J. Improved thermal conductivity of poly(dimethylsiloxane) composites filled with well-aligned hybrid filler network of boron nitride and graphene oxide. *Polym. Test* **2021**, *104*, 107402. [CrossRef]
13. Wang, J.; Ma, F.; Liang, W.; Sun, M. Electrical properties and applications of graphene, hexagonal boron nitride (h-BN), and graphene/h-BN heterostructures. *Mater. Today Phys.* **2017**, *2*, 6–34. [CrossRef]
14. Zhang, Z.; Liu, Y.; Yang, Y.; Yakobson, B.I. Growth Mechanism and Morphology of Hexagonal Boron Nitride. *Nano Lett.* **2016**, *16*, 1398–1403. [CrossRef] [PubMed]
15. Liu, S.; Wu, H.; Guo, S.; Qiu, J. Ordered stacking of oriented BN in confined space to construct effective heat transfer pathways. *Polymer* **2021**, *236*, 124300. [CrossRef]
16. Ge, X.; Chen, Y.; Liu, W.; Zhang, G.; Li, X.; Ge, J.; Li, C. Liquid cooling system for battery modules with boron nitride based thermal conductivity silicone grease. *RSC Adv.* **2022**, *12*, 4311–4321. [CrossRef]
17. Cheng, W.C.; Hsieh, Y.T.; Liu, W.R. Enhanced Thermal Conductivity of Silicone Composites Filled with Few-Layered Hexagonal Boron Nitride. *Polymers* **2020**, *12*, 2072. [CrossRef]
18. Padmanabhan Ramesh, V.; Sargolzaeiaval, Y.; Neumann, T.; Misra, V.; Vashaee, D.; Dickey, M.D.; Ozturk, M.C. Flexible thermoelectric generator with liquid metal interconnects and low thermal conductivity silicone filler. *NPJ Flex. Electron.* **2021**, *5*, 5. [CrossRef]
19. Available online: https://www.intertronics.co.uk/wp-content/uploads/2016/11/TB2007-12-Thermally-Conductive-Silicones.pdf (accessed on 12 June 2022).
20. Zhang, X.; Zhang, H.; Li, D.; Xu, H.; Huang, Y.; Liu, Y.; Wu, D.; Sun, J. Highly thermally conductive and electrically insulating polydimethylsiloxane composites prepared by ultrasonic-assisted forced infiltration for thermal management applications. *Compos. B Eng.* **2021**, *224*, 109207. [CrossRef]
21. Wang, J.; Huang, Q.; Li, X.; Zhang, G.; Wang, C. Experimental and numerical simulation investigation on the battery thermal management performance using silicone coupled with phase change material. *J. Energy Storage* **2021**, *40*, 102810. [CrossRef]
22. Cazacu, M.; Marcu, M. Silicone Rubbers. IX. Contributions to Polydimethylsiloxane-α,ω-Diols Synthesis by Heterogeneous Catalysis. *J. Macromol. Sci. A* **1995**, *32*, 1019–1029. [CrossRef]
23. Li, M.; Wang, M.; Hou, X.; Zhan, Z.; Wang, H.; Fu, H.; Lin, C.T.; Fu, L.; Jiang, N.; Yu, J. Highly thermal conductive and electrical insulating polymer composites with boron nitride. *Compos. B Eng.* **2020**, *184*, 107746. [CrossRef]
24. Zhang, H.; Shi, T.; Ma, A. Recent Advances in Design and Preparation of Polymer-Based Thermal Management Material. *Polymers* **2021**, *13*, 2797. [CrossRef] [PubMed]
25. Yang, D.; Wei, Q.; Yu, L.; Zhao, C.; Zhang, L. Enhanced thermal conductivity and mechanical properties of polymeric composites through formation of covalent bonds between boron nitride and rubber chains. *Polym. Adv. Technol.* **2021**, *33*, 212–220. [CrossRef]
26. Aradi, E.; Naidoo, S.R.; Billing, D.G.; Wamwangi, D.; Motochi, I.; Derry, T.E. Ion beam modification of the structure and properties of hexagonal boron nitride: An infrared and X-ray diffraction study. *Nucl. Instrum. Methods Phys. Res. B* **2014**, *331*, 140–143. [CrossRef]
27. Socrates, G. Infrared and Raman Characteristic Group Frequencies. In *Tables and Charts*, 3rd ed.; John Wiley and Sons: Hoboken, NJ, USA, 2004; pp. 94–246.
28. Yongnian, Z.; Bing, Z.; Zhi, H.; Yanchun, T.; Guangtian, Z. Infrared Spectroscopy Investigation of Cubic Boron Nitride Films. *Spectrosc. Lett.* **1998**, *31*, 945–954. [CrossRef]
29. Haque, A.; Narayan, J. Conversion of h-BN into c-BN for tuning optoelectronic properties. *Adv. Mater.* **2020**, *1*, 830–836. [CrossRef]
30. Pal, A.; Goswami, D.; Martinez, R.V. Elastic Energy Storage Enables Rapid and Programmable Actuation in Soft Machines. *Adv. Funct. Mater.* **2019**, *30*, 1906603. [CrossRef]
31. Pizzitutti, F.; Bruni, F. Electrode and interfacial polarization in broadband dielectric spectroscopy measurements. *Rev. Sci. Instrum.* **2001**, *72*, 2502. [CrossRef]
32. Samet, M.; Levchenko, V.; Boiteux, G.; Seytre, G.; Kallel, A.; Serghei, A. Electrode polarization vs. Maxwell-Wagner-Sillars interfacial polarization in dielectric spectra of materials: Characteristic frequencies and scaling laws. *J. Chem. Phys.* **2015**, *142*, 194703. [CrossRef]
33. Nishino, A. Capacitors: Operating principles, current market and technical trends. *J. Power Sources* **1996**, *60*, 137–147. [CrossRef]

34. Tugui, C.; Tiron, V.; Dascalu, M.; Sacarescu, L.; Cazacu, M. From ultra-high molecular weight polydimethylsiloxane to super-soft elastomer. *Eur. Polym. J.* **2019**, *120*, 109243. [CrossRef]
35. Kostoglou, N.; Polychronopoulou, K.; Rebholz, C. Thermal and chemical stability of hexagonal boron nitride (h-BN) nanoplatelets. *Vacuum* **2015**, *112*, 42–45. [CrossRef]
36. *Physical Property Measurement System, Thermal Transport Option User's Manual Part Number 1684-100B*; Quantum Design: San Diego, CA, USA, 2009.
37. Qu, J.; Fan, L.; Mukerabigwi, J.F.; Liu, C.; Cao, Y. A silicon rubber composite with enhanced thermal conductivity and mechanical properties based on nanodiamond and boron nitride fillers. *Polym. Compos.* **2021**, *42*, 4390–4396. [CrossRef]
38. Jiang, G.; Liu, T.; Liao, K.; Zhu, W. Effect of Micro-Scale and Nano-Scale Boron Nitride on Thermal Property of Silicone Rubber Via Experimental and Simulation Method. *Silicon* **2022**, *14*, 1969–1978. [CrossRef]
39. Xue, Y.; Li, X.; Wang, H.; Zhao, F.; Zhang, D.; Chen, Y. Improvement in thermal conductivity of through-plane aligned boron nitride/silicone rubber composites. *Mater Des.* **2019**, *165*, 107580. [CrossRef]
40. Dai, H.; Wang, R. Methods for Measuring Thermal Conductivity of Two-Dimensional Materials: A Review. *Nanomaterials* **2022**, *12*, 589. [CrossRef]